

Classical QGP : IV. Thermodynamics

Sungtae Cho and Ismail Zahed*

Department of Physics and Astronomy

State University of New York, Stony Brook, NY, 11794

Abstract

We construct the equation of a state of the classical QGP valid for all values of $\Gamma = V/K$, the ratio of the mean Coulomb to kinetic energy. By enforcing the Gibbs relations, we derive the pertinent pressure and entropy densities for all Γ . For the case of an SU(2) classical gluonic plasma our results compare well with lattice simulations. We show that the strongly coupled component of the classical QGP contributes significantly to the bulk thermodynamics across T_c .

arXiv:0812.1741v1 [nucl-th] 9 Dec 2008

*Electronic address: scho@grad.physics.sunysb.edu, zahed@zahed.physics.sunysb.edu

I. INTRODUCTION

Classical Plasmas are statistical systems with constituents that are locally charged but globally neutral. An example is the electromagnetic one component plasma (OCP) also referred to as Jelium. A number of many body theories have been devised to analyze the OCP in the regime of small $\Gamma = V/K$, the ratio of the average Coulomb energy to kinetic energy [1]. Most of the extensions to larger values of Γ are based on higher order transport equations [2] or classical molecular dynamics [3].

The Classical Quark Gluon Plasma (cQGP) as developed by Gelman, Shuryak and Zahed can be regarded as an extension of the OCP plasma to many components with non-Abelian color charges [4]. Stability against core collapse is enforced classically through a phenomenological core potential. The origin of the core is quantum mechanical. Detailed molecular dynamics simulations of the cQGP [4] have shown a strongly coupled plasma for $\Gamma = V/K \approx 1$ or larger. The cQGP maybe in a liquid state at moderate values of Γ . In a recent analysis [5] we have used analytical methods of classical liquids to construct the free energy for small Γ both in the dilute case and at high temperature after resummation of the screening effects.

In this paper we combine the results in [4] obtained from molecular dynamics with the one-loop analytical results in [5] to construct the equation of state of the cQGP for all values of Γ . We will show that the strongly coupled component of the cQGP contributes significantly to the thermodynamics across the transition whether in the energy density, pressure or entropy density. In section 2, we derive the excess energy of the cQGP for small Γ in the one-loop approximation. In section 3, we use ideas from classical electromagnetic plasmas to interpolate between the one-loop result at low Γ and the molecular dynamics results at large Γ for the SU(2) cQGP. Particular attention will be given to the core parameter using Debye-Hückel plus Hole (DHH) theory. In the quantum QCD plasma, Γ runs with T . In section 4, we use the interpolated excess energy density together with the Gibbs relations to derive the pressure and entropy of the cQGP. In section 5, we compare the results for the SU(2) cQGP with SU(2) lattice simulations. Our conclusions are in section 6. In Appendix A we show that the interaction corrections to the concentration do not affect the one-loop result to order $\Gamma^{\frac{5}{2}}$ with the bare particle concentration. In Appendix B we summarize the

Debye-Hückel plus Hole theory to assess the range of the core in terms of the Debye length.

II. EXCESS ENERGY: ONE-LOOP

In classical plasmas the key expansion parameter at zero chemical potential is $\Gamma = V/K$ the ratio of the mean Coulomb to kinetic energy. For an Abelian or QED plasma,

$$\Gamma = \frac{(Ze)^2}{ak_B T} \quad (\text{II.1})$$

while for a non-Abelian or QCD plasma [4]

$$\Gamma = \frac{g^2}{4\pi T a_{WS}} \frac{C_2}{a_{WS}} \quad (\text{II.2})$$

with $k_B = 1$ and a_{WS} the Wigner-Seitz radius satisfying $N/V(4\pi a_{WS}^3/3) = 1$. C_2 is the quadratic Casimir ($C_2 = q_2/(N_c^2 - 1)$) and g is the strength of the coupling. In the cQGP g is fixed, while in the QGP g runs with temperature. The running is quantum mechanical and beyond the present classical analysis. In sections 4,5 it will be addressed phenomenologically.

Since the Wigner-Seitz radius a_{WS} is tied with the density or concentration (the bare concentration is $c_0 = N/V$), it is straightforward to express the free energy in terms of Γ . After resumming the screening effects and to one-loop, the free energy reads [5]

$$\beta \frac{F_{loop}(\beta, c)}{V} = -c - \frac{2\sqrt{\pi}}{3}(N_c^2 - 1)\gamma^{\frac{3}{2}}c^{\frac{3}{2}} + \pi(N_c^2 - 1)c^2\gamma^2\sigma - 2\pi^{\frac{3}{2}}(N_c^2 - 1)c^{\frac{5}{2}}\gamma^{\frac{5}{2}}\sigma^2 + c\beta\mu_c + \mathcal{O}(\beta^3) \quad (\text{II.3})$$

with $\gamma = g^2/4\pi\beta C_2$, c the concentration and σ the core radius. The concentration is determined by the chemical equation [5] and to leading order is $c_0 = N/V$ as detailed in Appendix A. The core σ is a parameter in the cQGP much like in normal classical liquids. Its origin is quantum mechanical. In Appendix B, we use the classical Debye-Hückel plus Hole (DHH) theory to assess the size of the core in terms of the Debye screening length.

To see how the expansion in the concentration c in (II.3) converts to an expansion in Γ , we note that the Debye-Hückel contributions (first two terms) can be rewritten as

$$\frac{F_{DH}(\Gamma)}{NT} = -c\frac{V}{N} - c^{\frac{3}{2}}\frac{V}{N}\frac{2\sqrt{\pi}}{3}\left(\frac{g^2}{4\pi}\right)^{\frac{3}{2}}(N_c^2 - 1)(\beta C_2)^{\frac{3}{2}}$$

$$\begin{aligned}
&= -1 - c^{\frac{3}{2}} \frac{4\pi}{3} a_{WS}^3 \frac{(4\pi)^{\frac{1}{2}}}{3} \left(\frac{g^2}{4\pi}\right)^{\frac{3}{2}} (N_c^2 - 1) (\beta C_2)^{\frac{3}{2}} \\
&= -1 - \frac{1}{\sqrt{3}} c^{\frac{3}{2}} \left(\frac{4\pi a_{WS}^3}{3}\right)^{\frac{3}{2}} (N_c^2 - 1) \left(\frac{g^2}{4\pi} \beta \frac{C_2}{a_{WS}}\right)^{\frac{3}{2}} \\
&= -1 - \frac{1}{\sqrt{3}} (N_c^2 - 1) \Gamma^{\frac{3}{2}}
\end{aligned} \tag{II.4}$$

By defining the excess free energy F_{ex} as $F_{ex}(\Gamma) = F(\Gamma) - F(0)$ we obtain to one-loop,

$$\frac{F_{loop,ex}}{NT} = -\frac{1}{\sqrt{3}} (N_c^2 - 1) \Gamma^{\frac{3}{2}} + \frac{3}{4} \delta (N_c^2 - 1) \Gamma^2 - 3\sqrt{3} \delta^2 (N_c^2 - 1) \Gamma^{\frac{5}{2}} + \mathcal{O}(\Gamma^3) \tag{II.5}$$

with $\delta = \sigma/a_{WS}$. $F(0)$ will be identified with the free gas or Stephan-Boltzman contribution.

The excess energy U_{ex} of the cQGP follows from the excess free energy F_{ex} as

$$\frac{F_{ex}(\Gamma)}{NT} = \int_0^\Gamma \frac{U_{ex}}{NT} \frac{d\Gamma'}{\Gamma'} \tag{II.6}$$

For instance, the Debye-Hückel contribution in (II.7) yields through (II.6) the excess energy

$$\frac{U_{DH,ex}}{NT} = -\frac{\sqrt{3}}{2} (N_c^2 - 1) \Gamma^{\frac{3}{2}} \tag{II.7}$$

in agreement with the Debye-Hückel excess energy for the cQGP initially discussed in [6] using different methods. In general, the energy density splits into the free plus excess the contribution

$$\epsilon(\Gamma) = \frac{U(\Gamma)}{V} = \frac{U_0}{V} + \frac{U_{ex}(\Gamma)}{V} = \epsilon_0 + \epsilon(\Gamma) \tag{II.8}$$

with the free contribution $\epsilon_0 = \epsilon_{SB}$ identified with the Stefan-Boltzmann energy density ϵ_{SB} .

In relative notations,

$$\frac{\epsilon(\Gamma)}{\epsilon_{SB}} = 1 + \frac{1}{\epsilon_{SB}} \frac{U_{ex}(\Gamma)}{V} \tag{II.9}$$

Using (II.6) together with (II.5), we obtain the one-loop excess energy density

$$\frac{U_{loop,ex}}{NT} = -\frac{\sqrt{3}}{2} (N_c^2 - 1) \Gamma^{\frac{3}{2}} + \frac{3}{2} \delta (N_c^2 - 1) \Gamma^2 - \frac{15}{2} \sqrt{3} \delta^2 (N_c^2 - 1) \Gamma^{\frac{5}{2}} + \mathcal{O}(\Gamma^3) \tag{II.10}$$

which is valid for small Γ . In Appendix A, we show that although the concentration c in Γ is not c_0 because of interactions, to order $\Gamma^{5/2}$ we may set $c = c_0$.

III. EXCESS ENERGY: FULL

In [5] the one-loop expansion was shown to converge up to $\Gamma \approx 1$ for the free energy. The range is even smaller for the energy with $\Gamma \approx 1/2$ (see below). Larger values of Γ have been covered by molecular dynamics simulations in [4]. For an SU(2) plasma (say a constituent gluonic plasma) the numerical results for the excess energy were found to follow the parametric form [4]

$$\frac{U_{mol}}{NT} \simeq -4.9 - 2\Gamma + 3.2\Gamma^{\frac{1}{4}} + \frac{2.2}{\Gamma^{\frac{1}{4}}}. \quad (\text{III.1})$$

For $N_c = 2$ the one-loop result (II.10) reads

$$\frac{U_{anal}}{NT} = -\frac{3}{2}\sqrt{3}\Gamma^{\frac{3}{2}} + \frac{9}{2}\delta\Gamma^2 - \frac{45}{2}\sqrt{3}\delta^2\Gamma^{\frac{5}{2}} \quad (\text{III.2})$$

To construct the full excess energy valid for all Γ we will proceed phenomenologically by seeking an interpolating formulae between (III.1) and (III.2) borrowing from ideas in classical plasma physics [7]. A similar approach was also advocated in [8] using different limits.

In the Abelian or QED plasma, the excess energy based on Debye-Hückel theory is evaluated for $\Gamma < 0.1$. Molecular dynamics simulations are generated for $1 < \Gamma < 180$. The two are combined numerically through a power function in the form [7]

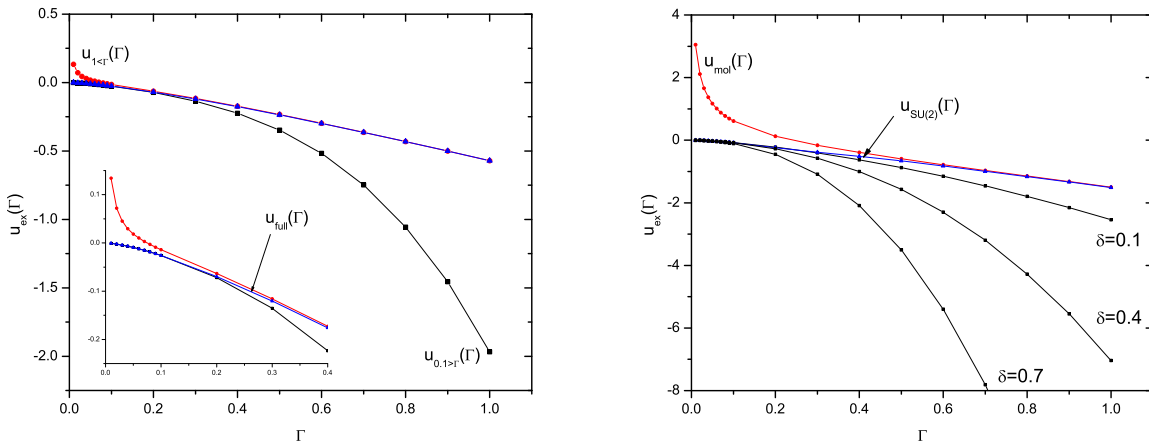


FIG. 1: Excess energy for QED (left) and $N_c = 2$ QCD (right)

$$u_{full}(\Gamma) = \frac{u_{\Gamma < 0.1}(\Gamma) + f(\Gamma)u_{\Gamma > 1}(\Gamma)}{1 + f(\Gamma)} \quad (\text{III.3})$$

with $f(\Gamma)$ a fitting power function of the type $a\Gamma^b (= 3.0 \times 10^3 \Gamma^{5.7})$. (III.3) interpolates smoothly between the exact analytical results at low Γ and the simulations at large Γ as shown in Fig. 1 (left). In the insert we show the nature of the size of the gap in the range $0.1 < \Gamma < 1$ for the Abelian plasma.

In Fig. 1 (right) we show our $N_c = 2$ results at low values of Γ (one-loop) and large values of Γ (simulations). The one-loop results depend on the size of the hard core σ . Recall that the simulations in [4] are carried with a fixed higher power law repulsion to mock up the core. So the simulations seem to favor a small hard core in the Wigner-Seitz units. In fact, σ can be set by the Debye radius in the DHH theory [9] detailed in Appendix B. It changes with Γ . Specifically,

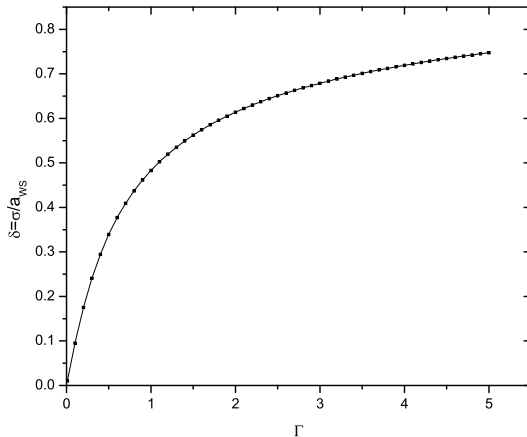


FIG. 2: Core parameter $\delta = \sigma / a_{WS}$. See text.

$$\delta = \frac{\sigma}{a_{WS}} = \frac{1}{a_{WS} \kappa_D} \left((1 + (3\Gamma)^{\frac{3}{2}})^{\frac{1}{3}} - 1 \right) = \frac{1}{(3\Gamma)^{\frac{1}{2}}} \left((1 + (3\Gamma)^{\frac{3}{2}})^{\frac{1}{3}} - 1 \right) \quad (\text{III.4})$$

which is shown in Fig. 2. The core size δ varies in the range $0.2 - 0.5$ for Γ in the range $0.1 - 1$. We fix $\delta = 0.4$ in the range $0.1 - 1$. With this in mind and following the Abelian plasma construction, we find the excess energies shown in Fig. 1 (right) to be fit by

$$u_{SU(2)}(\Gamma) = \frac{u_{anal}(\Gamma) + 5.5 \times 10^2 \Gamma^{5.4} u_{mol}(\Gamma)}{1 + 5.5 \times 10^2 \Gamma^{5.4}} \quad (\text{III.5})$$

The power function is numerically adopted to yield a small deviation (less than 0.1%) for $\Gamma < 0.1$ and $\Gamma > 1$. The precise choice of the core parameter is actually not very important, as small changes in core size can be compensated by small changes in the power function for the same overall accuracy.

IV. THERMODYNAMICS

Knowledge of the energy density for all values of Γ can be used to extract all extensive thermodynamical quantities in the cQGP with the help of the Gibbs relations. Indeed, the pressure and entropy follow from the Gibbs relations

$$\begin{aligned} \epsilon &= T \frac{\partial P}{\partial T} - P \\ s &= \frac{S}{V} = \frac{1}{V} \frac{\partial P}{\partial T} . \end{aligned} \quad (\text{IV.1})$$

In so far the classical plasma parameter Γ as defined (II.2) is a fixed parameter. However, in QCD it runs through α_s . It is only a function of temperature. Specifically,

$$\Gamma = \frac{\alpha_s C_2}{T a_{WS}} = \left(\frac{4\pi}{3} c_0 \right)^{\frac{1}{3}} \beta C_2 \alpha_s(T) = \left(0.244(N_c^2 - 1) \frac{4\pi}{3} \right)^{\frac{1}{3}} C_2 \alpha_s(T) \quad (\text{IV.2})$$

where $0.244(N_c^2 - 1)$ is the black-body concentration for adjoint gluons. The exact running of $\alpha_s(T)$ will be fixed below.

Using (IV.1) together with (IV.2) yield the pressure and the entropy density directly in terms of the energy density

$$\begin{aligned} \frac{P}{P_{SB}} &= 3 \frac{1}{T^3} \int_{T_c}^T dT' T'^2 \frac{\epsilon}{\epsilon_{SB}}(T') \\ \frac{s}{s_{SB}} &= \frac{3}{4} \frac{\epsilon}{\epsilon_{SB}}(T) + \frac{3}{4} \frac{1}{T^3} \int_{T_c}^T dT' T'^2 \frac{\epsilon}{\epsilon_{SB}}(T') . \end{aligned} \quad (\text{IV.3})$$

Here T_c is identified with the SU(2) transition with $P_c = 0$. For a constituent gluonic plasma $T_c = 215$ MeV. All bulk thermodynamics is tied to the energy density by the Gibbs relations.

V. SU(2) LATTICE COMPARISON

To proceed further we need to know how $\alpha_s(T)$ runs with T in pure YM and QCD, to determine the behavior of the extensive thermodynamical quantities. The loop expansion allows a specific determination of the running $\alpha_s(T)$ that is unfortunately valid at high temperature or weak coupling. How $\alpha_s(T)$ runs at strong coupling is unknown. Here we suggest to *extract* $\alpha_s(T)$ from the lattice data by *fitting* our energy density (II.9) valid for all couplings to the SU(2) lattice data in [10]. In Fig. 3 we show the fit of the normalized energy density in the cQGP to the SU(2) lattice data. The lattice results are used with $\Lambda_L = 5$ MeV and $T_c = 215$ MeV as suggested in [10].

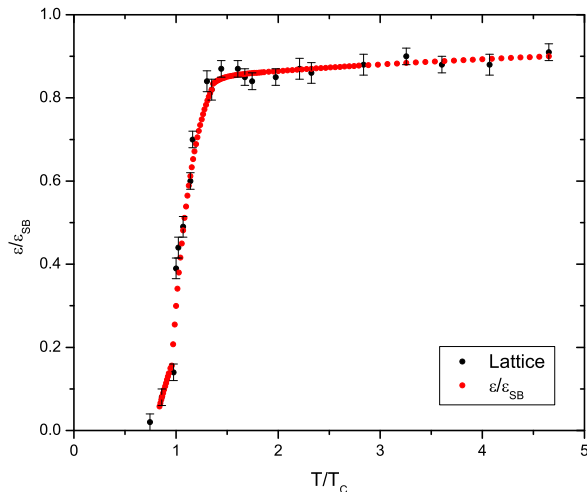


FIG. 3: Energy density fit to SU(2) lattice data. See text.

The energy density fit in return yields through (II.9), (III.5) and (IV.2) a specific running of the strong coupling constant $\alpha_s(T)$ which we show in Fig. 4 (left). Its corresponding running plasma constant $\Gamma(T)$ is shown in Fig. 4 (right). In Fig. 4 we also show two running coupling constants extracted from lattice measurements in [11] for comparison. Our energy density fit suggests lower values of the running coupling constant.

Since we have fit the energy density to the lattice energy density, to extract $\alpha_s(T)$, it follows from the Gibbs relations that all the extensive thermodynamical quantities are fixed for the SU(2) cQGP. In Fig. 5 (left) we show the behavior of the energy density, pressure

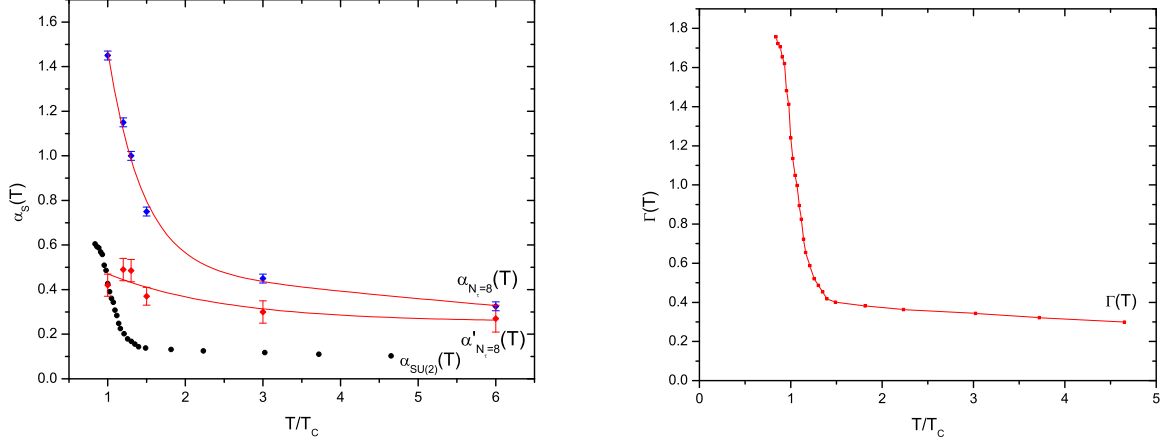


FIG. 4: $\alpha_s(T)$ (left) and $\Gamma(T)$ (right) for $N_c = 2$. See text.

and entropy density across T_c . In Fig. 5 (right) the trace of the energy momentum tensor is shown versus SU(2) lattice data.

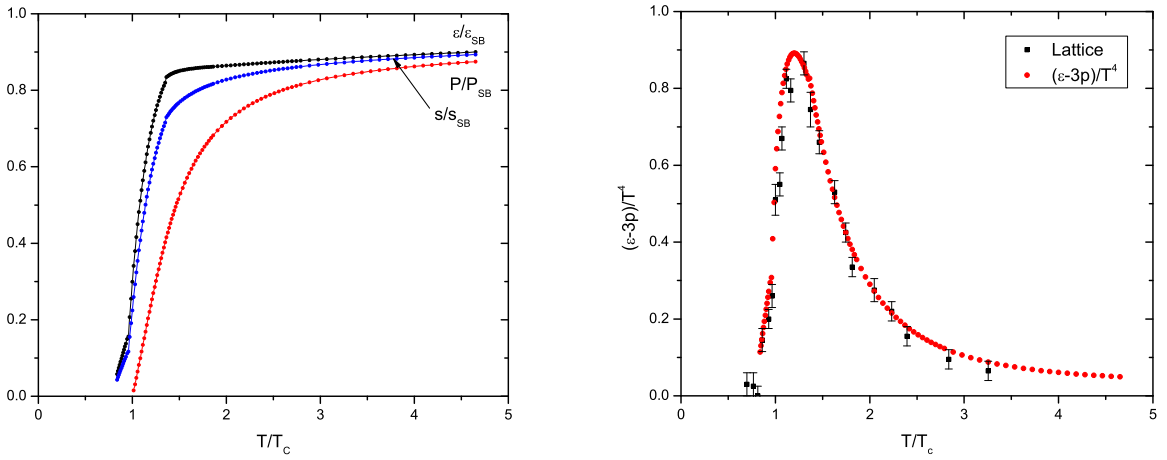


FIG. 5: Bulk Thermodynamics from the cQGP versus SU(2) lattice. See text.

Our current analysis of the bulk thermodynamics of the cQGP allows us through the excess energy (III.5) and the Gibbs relations (IV.1) to assess the role of the strongly coupled component of the cQGP. In Fig. 6 we show the two contributions (loop and molecular) to

the bulk thermodynamics following from the separation

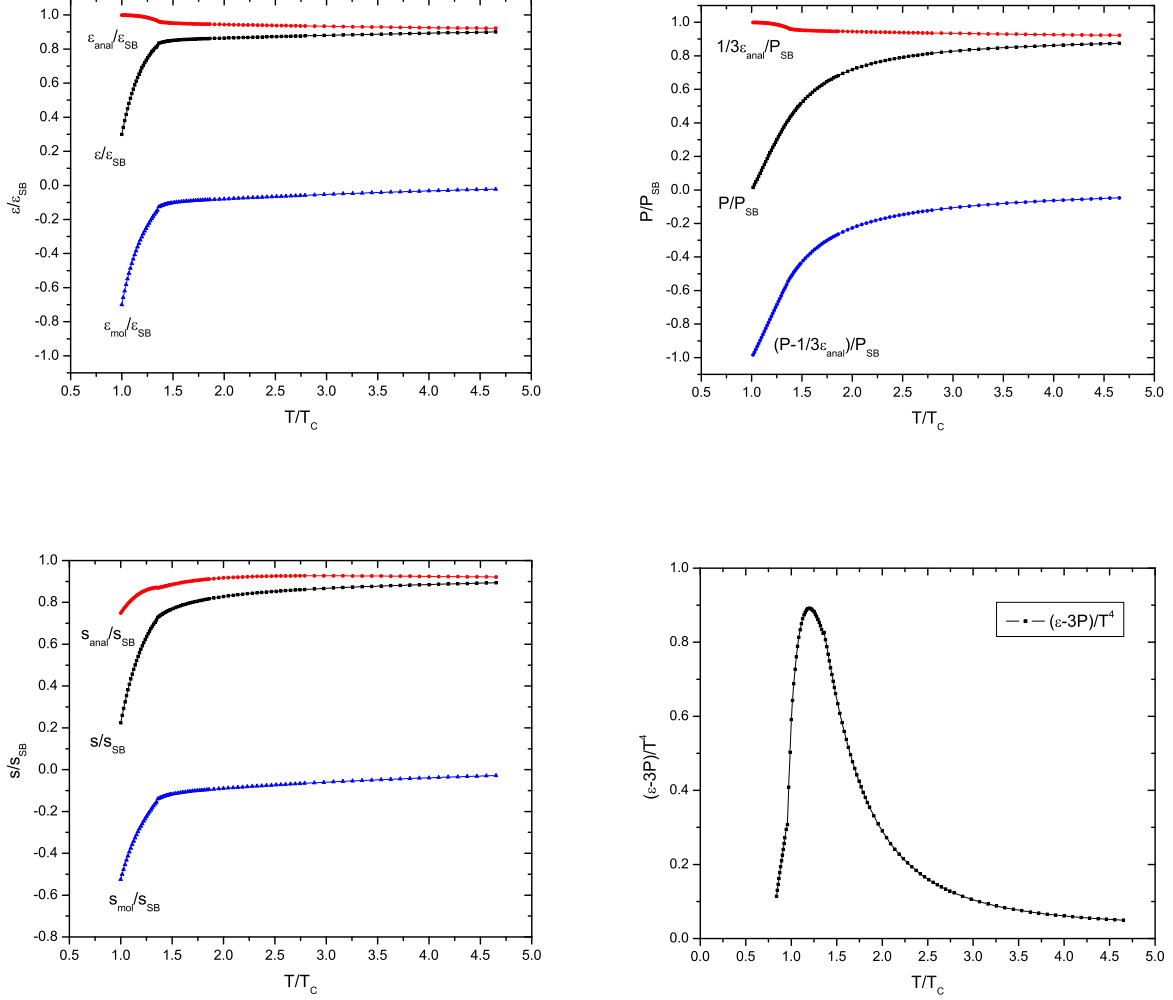


FIG. 6: Relative contributions in the cQGP bulk thermodynamics. See text.

$$\begin{aligned}
 u_{SU(2),anal}(\Gamma) &= \frac{u_{anal}(\Gamma)}{1 + 5.5 \times 10^2 \Gamma^{5.4}} \\
 u_{SU(2),mol}(\Gamma) &= \frac{5.5 \times 10^2 \Gamma^{5.4} u_{mol}(\Gamma)}{1 + 5.5 \times 10^2 \Gamma^{5.4}}
 \end{aligned}
 \tag{V.1}$$

in the energy density. The strongly coupled component of the cQGP generated by the molecular dynamics simulations contribute significantly across the transition temperature, say in the range $(1 - 2.5) T_c$.

VI. CONCLUSION

We have constructed the energy density of the cQGP valid for all values of the plasma parameter Γ , that interpolates between the one-loop result at small Γ and the molecular dynamics simulations at large Γ . We have used it in conjunction with the Gibbs relations to derive the Pressure and entropy of the cQGP.

In quantum QCD Γ runs through the QCD coupling constant at weak coupling. The running at strong coupling is unknown in general except for some recent lattice simulations [11]. We have suggested that a fit of our energy density to the lattice energy density [10] allows an extraction of the running coupling that is smaller than the one suggested by direct lattice simulations [11].

We have used the extracted running coupling constant to predict the entropy density, pressure and energy-momentum trace of the cQGP. The latter compares well to direct lattice SU(2) simulations. We have shown that the strongly coupled component of the cQGP contributes significantly to the bulk thermodynamics across the transition temperature. We expect transport properties such as diffusion and viscosity, as well as energy loss to be also significantly affected in this transition region in the cQGP as we discuss next [12].

VII. ACKNOWLEDGMENTS

This work was supported in part by US-DOE grants DE-FG02-88ER40388 and DE-FG03-97ER4014.

APPENDIX A: CONCENTRATION

The bare concentration $c_0 = N/V$ which is identified with the black-body radiation in the cQGP is in general modified to $c = c_0 + \Delta c$ due to interactions. As a result, the plasma parameter Γ (IV.2) is in principle different from the one used in the text. The corrected plasma constant is

$$\Gamma_c = \left(\frac{4\pi}{3}c\right)^{\frac{1}{3}}\beta C_2\alpha_s(T) = \left(\frac{4\pi}{3}(c_0 + \Delta c)\right)^{\frac{1}{3}}\beta C_2\alpha_s(T) = \left(\frac{4\pi}{3}c_0\right)^{\frac{1}{3}}\left(1 + \frac{\Delta c}{c_0}\right)^{\frac{1}{3}}\beta C_2\alpha_s(T)$$

$$\simeq \left(\frac{4\pi}{3}c_0\right)^{\frac{1}{3}}\beta C_2\alpha_s(T) + \left(\frac{4\pi}{3}c_0\right)^{\frac{1}{3}}\frac{1}{3}\frac{\Delta c}{c_0}\beta C_2\alpha_s(T) + \mathcal{O}\left(\left(\frac{\Delta c}{c_0}\right)^2\right) \quad (\text{A.1})$$

From [5], the shift in the concentration reads

$$c = c_0 + \Delta c = c_0 + c_0^{\frac{3}{2}}\pi^{\frac{1}{2}}(N_c^2 - 1)(\beta C_2)^{\frac{3}{2}}\alpha_s^{\frac{3}{2}}(T) + \mathcal{O}(\beta^2) \quad (\text{A.2})$$

The corrected plasma constant becomes

$$\begin{aligned} \Gamma_c &\simeq \left(\frac{4\pi}{3}c_0\right)^{\frac{1}{3}}\beta C_2\alpha_s(T) + \left(\frac{4\pi}{3}c_0\right)^{\frac{1}{3}}\frac{1}{3}c_0^{\frac{1}{2}}\pi^{\frac{1}{2}}(N_c^2 - 1)(\beta C_2)^{\frac{5}{2}}\alpha_s^{\frac{5}{2}}(T) \\ &= \Gamma + \frac{\sqrt{3}}{6}(N_c^2 - 1)\Gamma^{\frac{5}{2}} \\ &= \left(0.244(N_c^2 - 1)\frac{4\pi}{3}\right)^{\frac{1}{3}}C_2\alpha_s(T) + \frac{\sqrt{3}}{6}(N_c^2 - 1)\left(0.244(N_c^2 - 1)\frac{4\pi}{3}\right)^{\frac{1}{3}\cdot\frac{5}{2}}C_2^{\frac{5}{2}}\alpha_s^{\frac{5}{2}}(T) \end{aligned} \quad (\text{A.3})$$

Inserting (A.3) in the excess energy density yields

$$\begin{aligned} \frac{U_{loop,ex}(\Gamma)}{\epsilon_{SB}} &= -\frac{\sqrt{3}}{2}(N_c^2 - 1)\Gamma_c^{\frac{3}{2}} + \frac{3}{2}\delta(N_c^2 - 1)\Gamma_c^2 - \frac{15}{2}\sqrt{3}\delta^2(N_c^2 - 1)\Gamma_c^{\frac{5}{2}} + \mathcal{O}(\Gamma_c^3) \\ &\simeq -\frac{\sqrt{3}}{2}(N_c^2 - 1)\left(\Gamma + \frac{\sqrt{3}}{6}(N_c^2 - 1)\Gamma^{\frac{5}{2}}\right)^{\frac{3}{2}} + \frac{3}{2}\delta(N_c^2 - 1)\left(\Gamma + \frac{\sqrt{3}}{6}(N_c^2 - 1)\Gamma^{\frac{5}{2}}\right)^2 \\ &\quad - \frac{15}{2}\sqrt{3}\delta^2(N_c^2 - 1)\left(\Gamma + \frac{\sqrt{3}}{6}(N_c^2 - 1)\Gamma^{\frac{5}{2}}\right)^{\frac{5}{2}} \\ &\simeq -\frac{\sqrt{3}}{2}(N_c^2 - 1)\Gamma^{\frac{3}{2}} + \frac{3}{2}\delta(N_c^2 - 1)\Gamma^2 - \frac{15}{2}\sqrt{3}\delta^2(N_c^2 - 1)\Gamma^{\frac{5}{2}} + \mathcal{O}(\Gamma^3) \end{aligned} \quad (\text{A.4})$$

which shows that to order $\Gamma^{\frac{5}{2}}$ the replacement $\Gamma_c = \Gamma$ is allowed.

APPENDIX B: DEBYE-HÜCKEL PLUS HOLE (DHH) THEORY

At strong coupling the Debye-Hückel (DH) theory which is essentially a classical screening theory fails. Debye-Hückel plus Hole (DHH) theory is a way to address DH shortcomings at strong coupling by building a hole around each charge to account for the non-penetrability or core in classical liquids [9] at higher density or larger Γ . As a result, in DHH theory of the cQGP a color charge density around a test charge is

$$\rho^\alpha(r) = \begin{cases} -c \frac{g}{\sqrt{4\pi}} Q^\alpha & (r < \sigma) \\ -c \frac{g}{\sqrt{4\pi}} Q^\alpha \frac{\sigma}{r} e^{(-\kappa_D(r-\sigma))} & (r \geq \sigma) \end{cases} \quad (\text{B.1})$$

σ is the size of the hole, α is a classical color index ($1, \dots, N_c^2 - 1$), $\beta = 1/T$ and κ_D is the Debye momentum

$$\kappa_D^2 = \frac{g^2}{N_c^2 - 1} c \beta \sum_{\alpha}^{N_c^2 - 1} Q^{\alpha^2}. \quad (\text{B.2})$$

The negative sign in (B.1) reflects on the screening, with the Debye cloud left unchanged outside σ . The hole size σ is fixed by demanding that each test particle is completely screened through

$$\int_0^\infty dr 4\pi r^2 \rho^\alpha(r) = -\frac{g}{\sqrt{4\pi}} Q^\alpha \quad (\text{B.3})$$

This condition, fixes the size of the hole

$$\sigma = \frac{1}{\kappa_D} \left(\left(1 + \frac{3\kappa_D^3}{4\pi c} \right)^{\frac{1}{3}} - 1 \right) \quad (\text{B.4})$$

In terms of

$$\Gamma = \frac{g^2}{4\pi T a_{WS}} \quad (\text{B.5})$$

the hole radius is

$$\sigma = \frac{1}{\kappa_D} \left(\left(1 + (3\Gamma)^{\frac{3}{2}} \right)^{\frac{1}{3}} - 1 \right) \quad (\text{B.6})$$

after fixing the Wigner-Seitz radius a_{WS} through $c_0(4\pi a_{WS}^3/3) = 1$. Again we have set $c = c_0$. From (B.6) it follows that the hole size is smaller the higher the density or temperature.

-
- [1] S.Ichimarū, Rev. Mod. Phys. **54**, 1017 (1982)
[2] J.Hansen and I.McDonald, *Theory of Simple Liquids* (Academic Press, 2006)
[3] J.Hansen, I.McDonald and E.Pollock, Phys. Rev. A **11**, 1025 (1975)
[4] B.A.Gelman, E.V.Shuryak and I.Zahed, Phys. Rev. C **74**, 044908 (2006)
[arXiv:nucl-th/0601029]

- [5] S.Cho and I.Zahed [arXiv:0812.1736]
- [6] B.A.Gelman, E.V.Shuryak and I.Zahed, Phys. Rev. C **74**, 044909 (2006)
[arXiv:nucl-th/0605046]
- [7] S.Ichimarū, *Statistical Plasma Physics Vol II:Condensed Plasmas* (Westview Press, 2004)
- [8] V.Bannur, Eur. Phys. J. C **11**, 169 (1999) [arXiv:hep-ph/9811397]
- [9] S.Nordholm, Chem. Phys. Lett. **105**, 302 (1984)
- [10] J.Engels, F.Karsch and H.Satz, Phys. Lett. B **101**, 89 (1981)
- [11] O.Kaczmarek, F.Karsch, F.Zantow and P.Petreczky, Phys. Rev. D **70**, 070405 (2004)
[arXiv:hep-lat/0406036]
- [12] S. Cho and I. Zahed, in preparation.